



Pergamon

Acta Materialia 50 (2002) 4995–5004



www.actamat-journals.com

Modeling of graphitization kinetics during peritectic melting of tungsten carbide

Marios D. Demetriou *, Nasr M. Ghoniem, Adrienne S. Lavine

University of California, Mechanical & Aerospace Engineering Department, 91125 Pasadena, CA, USA

Received 22 April 2002; received in revised form 17 July 2002; accepted 19 July 2002

Abstract

A dynamic computational model developed within the context of the classical theory of phase evolution is applied to the W–C system to simulate the kinetics of graphite nucleation during non-equilibrium peritectic melting of WC. The kinetic variables used in the model are obtained directly from the free energy formulations that characterize the stable and metastable equilibria between WC, liquid, and graphite. The isothermal kinetic analysis suggests that transformation time decreases monotonically with increasing superheat such that the minimum transformation time occurs at the metastable congruent melting point of WC (~ 3107 K). To crystallize 1 ppm of graphite, the minimum transformation time is computed to be ~ 2 ns. The non-isothermal kinetic analysis suggests that under moderate to high heating rates (10^4 – 10^6 K/s) graphitization is completed at superheats of 40–50 K, while under ultra-high heating rates ($\sim 10^8$ K/s) graphitization remains incomplete giving rise to metastable congruent melting of WC.

© 2002 Acta Materialia Inc. Published by Elsevier Science Ltd. All rights reserved.

Keywords: Non-equilibrium processing; Nucleation; Growth; Cluster dynamics; Computer simulation

1. Introduction

Peritectic melting is a triple-point transition via which a peritectic phase β decomposes into liquid and a primary phase α , i.e., $\beta \rightarrow liq + \alpha$. It constitutes a particularly interesting kinetic scenario as it evolves under non-equilibration that is realized upon superheating rather than upon supercooling. Peritectic melting reactions are utilized in the processing of superconductors [1,2,3,4]. Kim et al. [5] experimentally investigated the decomposition kin-

etics of $Y_1Ba_2Cu_3O_{7-y}$ via a peritectic melting reaction. They observed the reaction to initiate by nucleation of primary particles directly at the advancing melting interface, and to progress by growth of the primary phase toward the interior of the dissolving peritectic phase. To date, no effort in modeling peritectic–melting kinetics was reported.

According to Perepezko and Boettinger [6], metastable equilibria of incongruently melting (peritectic) compounds form a congruent melting point that is masked by the equilibrium phase diagram. Upon superheating β , the peritectic melting reaction $\beta \rightarrow liq + \alpha$ is kinetically limited by the nucleation of α , and depending on the degree of superheat, the reaction may be suppressed such that

* Corresponding author. Fax: +1-626-795-6132.

E-mail address: marios@caltech.edu (M.D. Demetriou).

β coexists with the melt in metastable equilibrium. Moreover, under continuous heating conditions such as those encountered in rapid thermal processing, the stable peritectic melting reaction could be kinetically bypassed giving rise to metastable congruent melting of β .

The tungsten–carbon (W–C) system at carbon composition of 50%, which corresponds to the composition of the peritectic compound tungsten carbide (WC), will be considered in this study as a sample compound-forming system to analyze the kinetics of peritectic melting by means of the developed model. The choice for the W–C system is attributed to the fact that the W–C thermodynamic properties are very well documented [7], and to the fact that the WC peritectic compound is attractive for barrier thermal coating applications due to its good thermal and chemical stability, high hardness, and high oxidation resistance, and is widely processed by means of rapid thermal processing techniques. Rapid thermal processing of WC often involves rapid heating and melting of WC, which is accomplished by means of high-energy beam sources such as plasma, ion, electron, or laser. Under such non-equilibrium melting conditions, the rate of the stable peritectic reaction via which WC peritectically decomposes into liquid and graphite, i.e. $WC \rightarrow liq + gra$, would be limited by the nucleation kinetics of graphite. Moreover, it is postulated that a critical heating rate may exist under which graphite will fail to nucleate sufficiently and consequently WC will melt via the metastable congruent reaction $WC \rightarrow liq$. Under such extreme conditions metastability will prevail, as graphite would be kinetically bypassed.

Attempting to experimentally analyze the kinetics of such transition could be a challenging task as the kinetic rate is expected to be extremely high owing to enhanced mobility at high temperatures. The kinetics can be experimentally investigated by monitoring crystallization events during laser-beam heating of a WC thin film by means of differential thermal analysis or differential scanning calorimetry. However, the response time of such methods could be rather long compared to the kinetic time scales involved in the transition, hence the instruments' reading would be rather unreliable. Therefore, more advanced experimental

methods would be required such as high-speed x-ray diffraction analysis and in-situ resistivity measurements [8]. The sophistication required in monitoring such fast kinetics renders kinetic modeling an attractive alternative, as it may provide a fairly accurate quantitative assessment of the processing kinetics.

In this study, a computational model is developed to simulate the kinetics of graphite nucleation upon WC superheating. The aim is to assess the importance of nucleation kinetics in limiting the rate of peritectic melting reaction. This study constitutes the first attempt to model nucleation kinetics in peritectic melting. The present model, which was developed in the context of classical nucleation theory, simulates the stochastic process of crystal nucleation by modeling the dynamics of cluster evolution. The model also accounts for size-dependent growth of finite size nuclei. The kinetic variables used in the model were obtained directly from the free energy formulations that characterize the stable and metastable equilibria between WC, liquid, and graphite. The empirical relations that govern kinetic properties under conditions of supercooling are adopted in the present model and are extrapolated above equilibrium to approximate properties under superheating conditions. Furthermore, de-carburization was neglected and fixed composition at 50%-C was assumed throughout the process. The model was applied to investigate the kinetics of graphite nucleation via the stable peritectic reaction $WC \rightarrow liq + gra$ upon annealing or continuous heating, and to examine the possibility of complete kinetic bypassing of the graphite phase.

2. Thermodynamic modeling

Demetriou et al. [9] developed a CALPHAD algorithm to compute the metastable W–C phase diagram in the vicinity of the metastable reactions involving the carbides by reproducing the equilibrium boundaries using optimized free energy data obtained from [7], and by extending the stable boundaries into regions of metastability as suggested by [6]. The computed stable phase equilibria are in excellent agreement with those computed by

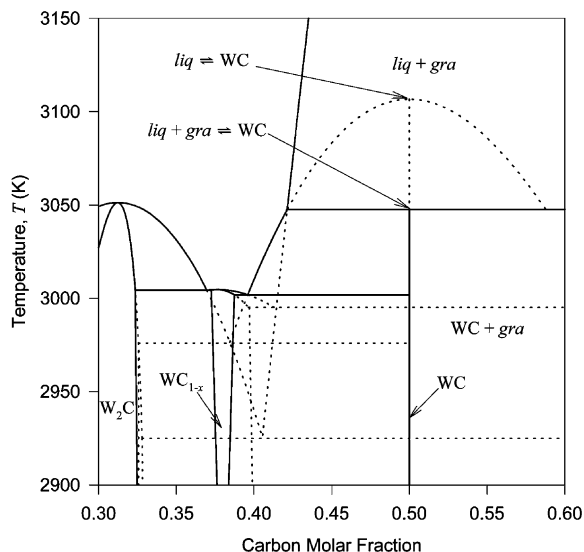


Fig. 1. The computed stable and metastable W–C phase diagram [7, 8].

[7], which closely resemble experimental phase equilibrium data presented by [10]. The computed phase diagram with the metastable equilibria superimposed as dotted lines is shown in Fig. 1. The thermodynamically stable peritectic reaction and the metastable congruent reaction at 50%–C are designated in Fig. 1, and are tabulated in Table 1 along with the corresponding equilibrium compositions and temperatures. The metastable phase diagram suggests that the equilibrium peritectic melting reaction $WC \rightarrow liq + gra$ takes place at 3047 K, while the metastable congruent melting reaction $WC \rightarrow liq$ occurs at 3106 K. The reaction enthalpy and entropy associated with each of these transitions, ΔH_f and ΔS_f , are evaluated from the free energy functions and are also listed in Table 1.

The supersaturation of graphite $\Delta\mu$, which constitutes the driving force for graphite nucleation, is

the free energy change associated with nucleating one molecule of graphite out of the metastable liq – WC equilibrium [11]. The graphite supersaturation is computed directly from the free energy formulations that characterize the liq , WC , and gra phases and is plotted in Fig. 2 in the range of 3047 K (the equilibrium peritectic temperature) to 3106 K (the metastable congruent melting point of WC). As expected, the $\Delta\mu$ vs. T plot, which quantifies the thermodynamic stability of gra with reference to the liq – WC equilibrium at 50%–C, suggests that graphite supersaturation increases with temperature in a highly exponential fashion and is maximized at the metastable congruent melting point. At temperatures higher than the congruent point (not shown in the graph), the supersaturation of graphite decreases linearly with temperature and dimin-

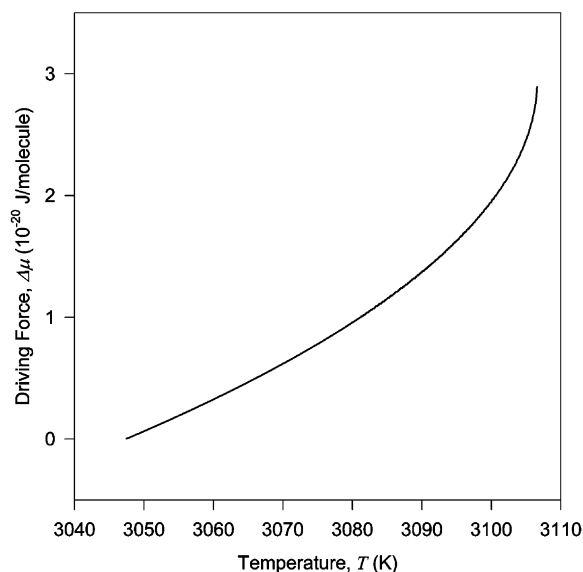


Fig. 2. Thermodynamic driving force for graphite nucleation out of the liq – WC equilibria upon superheating at 50%–C vs. temperature.

Table 1
Stable and metastable equilibria among participating phases

Reaction	Reaction type	Carbon Molar Fraction	Temperature T (K)	Reaction Enthalpy ΔH_f (kJ/mol)	Reaction Entropy ΔS_f (J/mol-K)
$liq + gra \rightleftharpoons WC$	Peritectic	0.421 0.500 1.00	3047	60.48	19.86
$liq \rightleftharpoons WC$	Congruent	- 0.500 -	3107	77.72	25.03

ishes at the graphite liquidus (~3583 K). It is therefore postulated that unless sufficient nucleation takes place between 3047 and 3106 K, the graphite phase will not evolve but rather dissolve and consequently it will be bypassed.

3. Kinetic analysis

In order to assess whether metastability would prevail in a peritectic melting reaction, i.e., whether the overwhelming kinetics of metastable congruent melting would completely suppress the nucleating phase, the criterion proposed by Hunziker et al. [12] was adopted. The criterion states that the nucleation density of a phase nucleating at a triple point needs to be high enough such that the volume ahead of the growing interface is rapidly filled with the nucleating phase. Thus, the kinetic analysis in this study will be conducted in terms of surface nucleation over an established melting interface, and metastability will be assessed by determining whether the nucleating phase has surface-crystallized substantially to thwart metastable melting.

For the reaction path $WC \rightarrow liq + gra$, a moving melting interface between liquid and WC may be assumed over which graphite nuclei emerge. However, in a nucleation time frame, this interface may be treated as stationary since its kinetics are diffusion-limited and are characterized by long time scales. Owing to the strong interfacial tensions at the crystal–crystal interface the graphite nuclei are more likely to emerge in the liquid side of the interface rather than in the WC side. Furthermore, since atomic mobility in the liquid is anticipated to be significantly greater than in the solid, transport of monomers (carbon atoms) will take place predominantly in the liquid. Accordingly, from a kinetic point of view, the liquid can be regarded as the parent phase while the primary solid can be treated as a stationary and inert substrate over which nuclei are catalyzed. The geometry of such triple-point transition can be modeled as a catalyzed reaction as illustrated in Fig. 3.

In catalyzed nucleation reactions, the wetting angle θ can be correlated with the melting temperatures of the two participating solid phases [13]. The

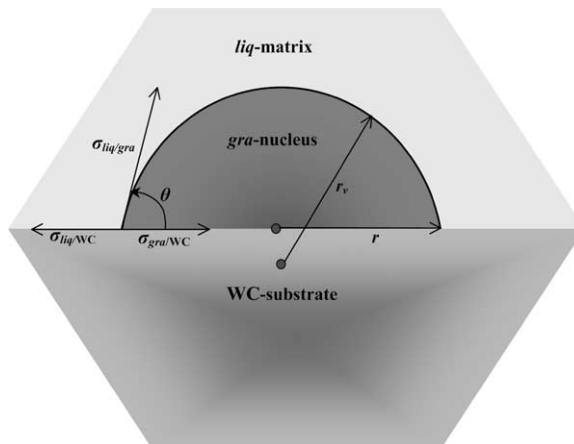


Fig. 3. The geometry of a triple-point reaction: a *gra*-phase cluster nucleates in *liq* matrix over a WC-phase catalytic substrate.

wetting angle for the $WC \rightarrow liq + gra$ reaction was evaluated to be 37° . As the nucleating graphite phase is unary, the cluster dimension can be represented by a single size coordinate n that would denote the number of clustered carbon atoms. The availability of monomeric sites that would contribute to a unit surface of product phase, i.e., the initial number of available carbon atoms in the liquid per unit surface of nucleated graphite, can be approximated as $N^i \sim (fV_m)^{-2/3}$, where V_m is the graphite molecular volume and f is the graphite phase fraction obtained from the lever rule. The relationship between the size of a cluster of n atoms and its surface radius r , as shown in Fig. 3, is:

$$r(n) = \sin\theta \left[\frac{3V_m}{4\pi f(\theta)} \right]^{1/3} n^{1/3} \quad (1)$$

where $f(\theta) = (2 + \cos\theta)(1 - \cos\theta)^2/4$. The liquid–crystal interfacial area is given by $A_n = (36\pi)^{1/3} [f(\theta)]^{1/3} V_m^{2/3} n^{2/3}$ while the number of interfacial atomic sites is $O_n = 2(1 - \cos\theta)[f(\theta)]^{2/3} n^{2/3}$ [14].

The liquid–crystal interfacial energy during nucleation may be approximated by [11]:

$$\sigma_{liq/gr} \equiv \sigma = \frac{\alpha_m \Delta S_f T}{N_A V_m^{2/3}} \quad (2)$$

where N_A is Avogadro's number, ΔS_f is the equilib-

rium reaction entropy, and α_m is a structure-dependent factor. Eq. (2) assumes a purely entropic form of the interfacial energy by neglecting the contribution of higher order terms. Furthermore, it ignores the effect of compositional change at the interface. Nevertheless, in the context of this study the above relation was taken to be adequate in approximating liquid–crystal interfacial energy during peritectic melting. The equilibrium reaction entropy is taken to be 19.86 J/mol-K, which corresponds to the entropy of the equilibrium triple-point transition evaluated from free energy functions (see Table 1). The graphite molecular volume is taken as $8.796 \times 10^{-30} \text{ m}^3/\text{molecule}$. Also, for hexagonal graphite $\alpha_m \approx 0.77$ [15]. In the transformation range considered (3047–3106 K), the interfacial energy as estimated from Eq. (2) increases linearly with temperature between 1.81 and 1.85 J/m².

The unbiased molecular jump frequency at the cluster interface may be approximated by the jump rate in the bulk liquid. Assuming three-dimensional random walk process and the validity of Stokes–Einstein relationship, the jump rate γ can be related to the liquid viscosity η as:

$$\gamma = \frac{2k_B T}{\pi V_m \eta} \quad (3)$$

where k_B is the Boltzmann's constant. The temperature-dependent viscosity of the undercooled liquid was approximated using the iso-free volume model proposed by Battezzati et al. [16], and the composition dependence was incorporated as suggested by Moelwyn–Hughes [17]. The molecular jump frequency is estimated to be of order 10^{10} s^{-1} .

As the mobility in such high-temperature reaction is high, the barrier for monomeric units to diffuse from the bulk liquid to the cluster immediate vicinity is vanishingly small as compared to the attachment/detachment interfacial barrier. Hence the nearest-neighbor shell of a graphite cluster can be taken to have all available sites O_n filled with carbon atoms, which attach/detach to the cluster stochastically. On that account, the current problem can be reduced to that of partitionless nucleation, which can be modeled by the classical interface-limited cluster evolution theory. According to the classical theory, fluctuation in the forma-

tion of an n -size cluster is connected with the minimum reversible work needed for its formation, which can be expressed as the balance between volume and surface contributions as follows [18]:

$$\Delta G_n = -n\Delta\mu + A_n\sigma \quad (4)$$

where macroscopic (independent of n) values for $\Delta\mu$ and σ are assumed. A maximum in ΔG_n is obtained at a critical size $n^* = (32/3)\pi\sigma^3 V_m^2 f(\theta) / \Delta\mu^3$ as $\Delta G_{n^*} = (16/3)\pi\sigma^3 V_m^2 f(\theta) / \Delta\mu^2$, and is referred to as the critical activation energy. The critical activation energy for graphite nucleation in the temperature range of 3047 K to 3107 K is computed from Eq. (4) and is plotted in Fig. 4. The plot suggests that ΔG_{n^*} decreases monotonically with temperature in a highly exponential fashion, attaining $\sim 10^{-19}$ J at the congruent melting point.

4. Cluster dynamics

According to the rate theory of atomic clustering, nucleation can be modeled by a first-order kinetic equation that has the form of a master equation [18]:

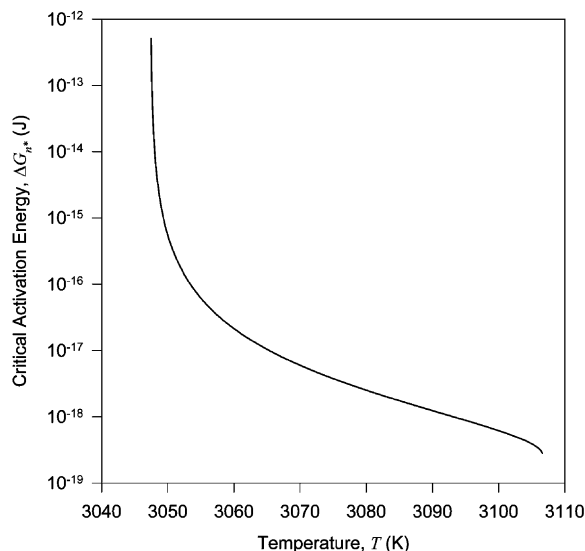


Fig. 4. Critical activation barrier for graphite nucleation during peritectic melting of WC.

$$\frac{dN_n(t)}{dt} = I_{n-1}(t) - I_n(t) = N_{n-1}(t)k_{n-1}^+ - [N_n(t)k_n^- + N_n(t)k_n^+] + N_{n+1}(t)k_{n+1}^- \quad (5)$$

where $N_n(t)$ is the time-dependent density of an n -size cluster, $I_n(t)$ is the time-dependent nucleation frequency at size n , k_n^+ is the rate of monomer attachment to an n -size cluster and k_n^- is the rate of monomer detachment given as:

$$k_n^+ = O_n \gamma \exp\left(-\frac{\Delta G_{n+1} - \Delta G_n}{2k_B T}\right) \quad (6a)$$

$$k_{n+1}^- = O_n \gamma \exp\left(-\frac{\Delta G_n - \Delta G_{n+1}}{2k_B T}\right) \quad (6b)$$

Stochastic evolution theory dictates that under static conditions (e.g., under constant temperature) a steady state cluster distribution would be established such that the nucleation rate becomes constant. This steady-state rate is given by:

$$I^s = \left(\sum_{n_{min}}^{n_{max}} \frac{1}{N_n^e k_n^+}\right)^{-1} \quad (7)$$

where n_{min} and n_{max} are a lower and upper size bound about n^* determined accordingly to ensure the accuracy of the simulation [18,19], and $N_n^e = N^i \exp(-\Delta G_n/k_B T)$ is the equilibrium cluster distribution. The evolution of cluster size distribution and the nucleation frequencies were obtained by solving the system of stiff, coupled differential equations given in Eq. (5) by means of a MATLAB stiff ODE solver calibrated to a relative tolerance of 10^{-3} that was supplied with the rate constants and with boundary and initial conditions.

The extended crystallized surface fraction, $x_e(t)$, can be established by accounting for the surface area of all supercritical clusters, i.e., $x_e(t) = \sum_{n > n^*} \pi[r(n)]^2 N_n(t)$. However, for clusters suf-

ficiently exceeding the critical size, the diffusion component of the nucleation rate characterizing size fluctuations becomes vanishingly small in relation to the drift component that accounts for deterministic growth. Hence, ignoring fluctuational growth for $n \gg n^*$, a growth law may be derived as $dn/dt \equiv k_n^+ - k_{n+1}^- \cong I_n(t)/N_n(t)$, where dn/dt is

the drift velocity or growth rate. Assuming a transition from fluctuational to deterministic growth at a post-critical size $n_{post} \gg n^*$, the growth law may be employed to yield a time-integral form of $x_e(t)$ [20]:

$$x_e(t) = \int_0^t \pi[r(t;t')]^2 I_{r_{post}}(t') dt' \quad (8)$$

The convolution function $r(t;t')$ denotes the size of a cluster at time t which nucleated at a time t' when $r(t') = r_{post}$. It can be obtained by solving the initial value problem governing the time evolution of a supercritical cluster:

$$\frac{dr}{dt} = \left(\frac{16V_m f(\theta)}{9\pi}\right)^{1/3} \sin\theta(1 - \cos\theta) \gamma \sinh\left(\frac{\Delta\mu - 2V_m \sigma \sin\theta/r}{2k_B T}\right) \quad (9)$$

In the limit of n being continuous, the steady-state nucleation rate I^s and the critical incubation time ϑ_{n^*} , were derived analytically by [21] as $I^s = z k_{n^*}^+ N_{n^*}^e$ and $\vartheta_{n^*} = 2/3 \pi k_{n^*}^+ z^2$ respectively, where $z = (\Delta\mu/6\pi k_B T n^*)^{1/2}$ is the Zeldovich factor. Taking the nucleation rate $I_{r_{post}}(t)$ to be relaxed at its steady state value I^s and assuming zero-size nuclei and infinitely large crystals, a quasi-steady form of the kinetic problem may be obtained as:

$$x_e(t) = \int_0^t \pi \left[\int_{t'}^t u(t'') dt'' \right]^2 I^s(t') dt' \quad (10)$$

where $u = (dr/dt)|_{r \rightarrow \infty}$. Under isothermal conditions the kinetics can be further reduced to $x_e(t) = \pi I^s u^2 t^3/3$. The time-dependent surface fraction transformed, $x(t)$, that accounts for the overlap of crystallites can be obtained from the Avrami statistical model [22] as $x(t) = 1 - \exp[-x_e(t)]$.

5. Isothermal kinetics

The effects of nucleation transience during isothermal (static) conditions become significant when the relaxation time ϑ_{n^*} becomes comparable

to the transformation time τ . A steady state kinetic model neglects these transient effects and consequently overestimates the kinetics. In the work of Demetriou [20], the transient effects during isothermal conditions for the reaction considered in this study were assessed by comparing the analytically evaluated ϑ_{n^*} to τ evaluated from a steady state kinetic model. In his work, transient effects were determined to be negligible for annealing between 3047 and 3090 K, but become important at higher temperatures, as the transformation time becomes comparable or smaller than the induction time. In order to warrant the accuracy of the simulation at all annealing temperatures considered, the isothermal transformation diagrams (TTT) were produced by means of the explicit dynamic simulation of cluster evolution outlined in Cluster Dynamics. For more details on the isothermal simulation refer to [19].

Isothermal crystallization during annealing at 3095 K (48 K superheating) will be considered as a sample case to demonstrate the results of the developed model. The annealing duration τ was taken to be 0.1 μs . The analytically evaluated induction time ϑ_{n^*} at 3095 K is ~ 20 ns, about five times smaller than τ . The time-dependent forward flux at n^* along with the one at n_{post} is plotted in Fig. 5. The forward flux at the critical size, $I_{n^*}(t)$, appears to attain its steady state value at $t' \approx 3\vartheta_{n^*}$, in accordance with the analytical treatment of Kashchiev [21]. The forward flux at the post-critical size however, $I_{n_{post}}(t)$, which can be regarded as the nucleation rate, remains transient throughout the transition and barely attains its steady state value at the end of the annealing. This plot therefore renders a steady state kinetic model that assumes a relaxed nucleation rate inadequate.

The time-dependent crystallized surface fraction $x(t)$ computed with means of a dynamic and a steady state model is plotted in Fig. 6. As expected, at early times (see insert in Fig. 6) when the nucleation rate is highly transient, the steady state model overestimates the rate of kinetics by several orders of magnitude. According to the steady state model 1-ppm crystallizes at ~ 14 ns, while according to the dynamic model 1-ppm crystallizes at ~ 22 ns. At later times when the nucleation rate approaches its steady state value, the results from

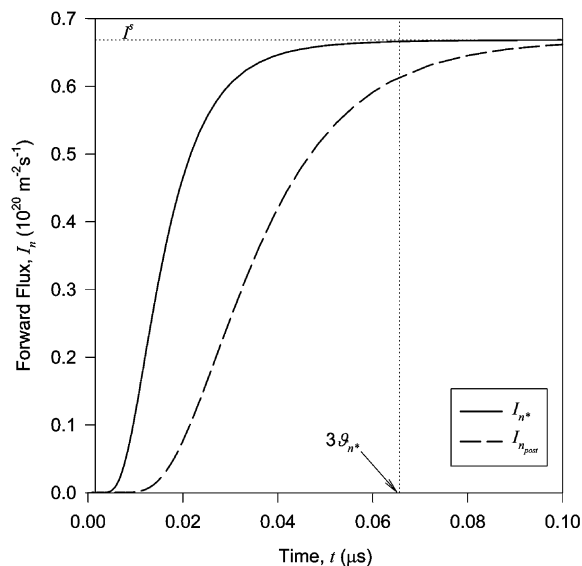


Fig. 5. Nucleation frequency of graphite vs. time during peritectic melting of WC upon annealing at 3095 K for 0.1 μs .

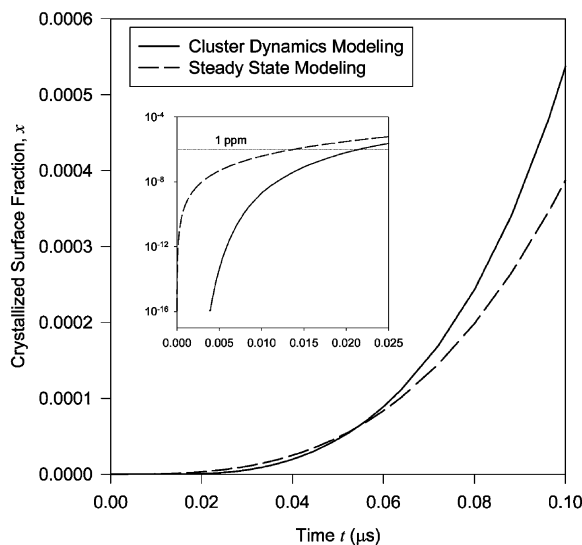


Fig. 6. Crystallized surface fraction of graphite vs. time during peritectic melting of WC upon annealing at 3095 K for 0.1 μs .

the two models converge to the same order of magnitude. Thus Fig. 6 suggests that at moderate superheating nucleation transience influences crystallization at early times, while at late times it has a negligible effect. The relatively small deviation in

the results of the two models at late times is attributed to the treatment of growth. In evaluating growth, the initial size of nucleated particles is neglected in the steady state model and as a result the rate of kinetics is slightly underestimated.

The isothermal transformation diagram (TTT curve) for this transition computed from dynamic and steady state models is shown in Fig. 7. The gradual deviation in the computed transformation time obtained from the two models, which becomes apparent at 3090 K and reaches several orders of magnitude by 3106 K, is clearly illustrated. This diagram quantitatively demonstrates the importance of nucleation transience in modeling isothermal crystallization kinetics under high superheating. Moreover, it verifies that the effects of transience can be accurately assessed by means of a simple time scale analogy as suggested by [20]. The TTT curve shown in Fig. 7 does not emulate the typical “nose” shape perceived in classical crystallization reactions under supercooling conditions. This is because in the peritectic melting reaction, non-equilibration is accomplished by superheating and as a result both interfacial activation barriers (diffusion and nucleation) decrease with increasing temperature. Accordingly, the nucleation and growth rates, and consequently the

crystallization rate, increase monotonically with temperature so that the minimum transformation time appears to occur at the metastable congruent melting point. The dynamic model suggests that the minimum transformation time for 1-ppm at the metastable congruent melting point is ~2 ns. Contrarily, the steady state model, which severely overestimates the kinetics at that temperature, predicts a transformation time of only ~84 ps.

6. Non-isothermal kinetics

Under dynamic (non-isothermal) conditions, transient effects attributed to the explicit dependence of the activation barriers on temperature may become significant when the barriers change sooner than it takes for nucleation to relax. Schneiderman [23] suggested that the limiting barrier rate of change in assessing the importance of transient effects during dynamic conditions appears to be that of nucleation. A time scale to characterize the rate of change of the nucleation barrier can be obtained as $\varphi_{n^*} = [d(-\Delta G_{n^*}/k_B T)/dt]^{-1}$. Owing to the temperature dependence of the activation barrier, φ_{n^*} becomes inversely proportional to the heating rate dT/dt . Hence, comparing this dynamic time scale to the induction time gives an indication of the importance of transient effects during dynamic conditions, i.e., transient effects can become important when $\varphi_{n^*} \ll \vartheta_{n^*}$. Demetriou [20] assessed the effects of transience upon dynamic conditions in the reaction considered in this study by comparing ϑ_{n^*} computed analytically to φ_{n^*} evaluated at different heating rates. According to such time scale analogy transient effects were determined to be important only under ultra-high heating rates of order 10^8 K/s. Therefore, in order to warrant the simulation accuracy at all heating rates considered, the non-isothermal crystallization kinetics were computed with means of a dynamic simulation. The non-isothermal simulation is discussed in detail in [19].

The transient nucleation frequency of post-critical clusters evaluated for different heating rates is plotted within the corresponding transformation range in Fig. 8. The temperature-dependent quasi-steady state rate is also plotted to accentuate transi-

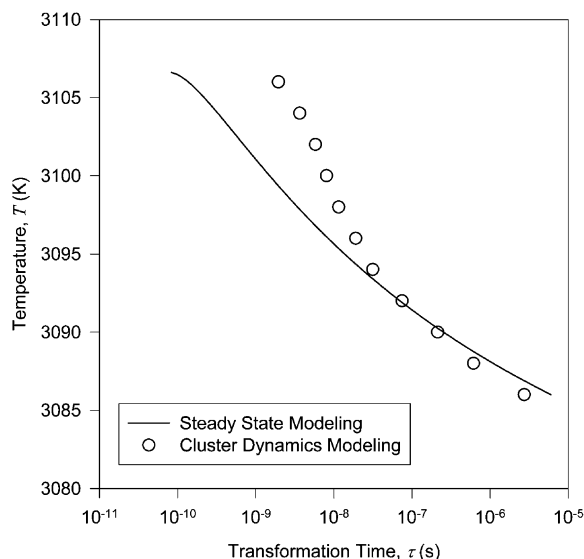


Fig. 7. Transient and steady state TTT diagrams for graphite crystallization during peritectic melting of WC for $x = 10^{-6}$.

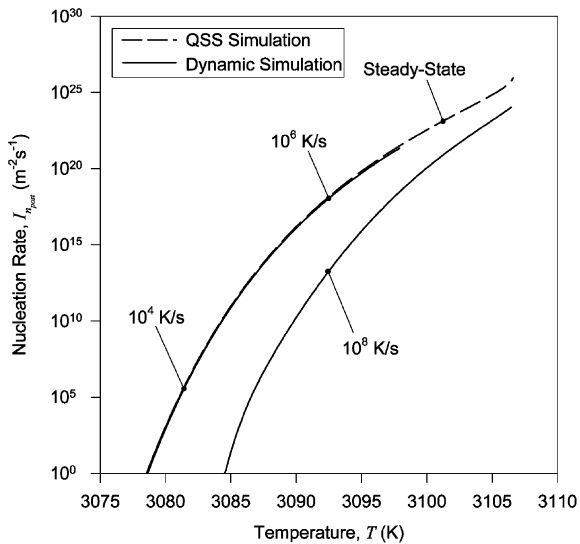


Fig. 8. Dynamic nucleation rate of graphite during peritectic melting of WC vs. temperature for various heating rates.

ence. For processing rates of 10^4 and 10^6 K/s, the transient nucleation frequency appears indistinguishable from the quasi-steady state rate. For 10^8 K/s, however, the results of the two models appear to deviate substantially, hence verifying the assessment of transience based on time scale analogy as suggested by [20].

The crystallization kinetics computed from the dynamic simulation along with those computed from the QSS simulation for 10^4 , 10^6 , and 10^8 K/s heating rates are shown in Fig. 9. As transient effects are insignificant for processing under 10^4 K/s and 10^6 K/s heating rate, the results of the two models appear almost indistinguishable. For processing under 10^8 K/s, however, the results of the two models deviate substantially as transient effects dominate the nucleation process. The continuous-heating transformation diagram in Fig. 9 quantitatively demonstrates the significance of nucleation transience in modeling non-isothermal crystallization kinetics under high heating rates. The kinetics computed dynamically suggest that under 10^4 K/s and 10^6 K/s heating rates, graphite transformation is completed at superheats of 43 K and 50 K respectively, while under 10^8 K/s the transformation remains incomplete by the time the WC-substrate melting point is attained. The meta-

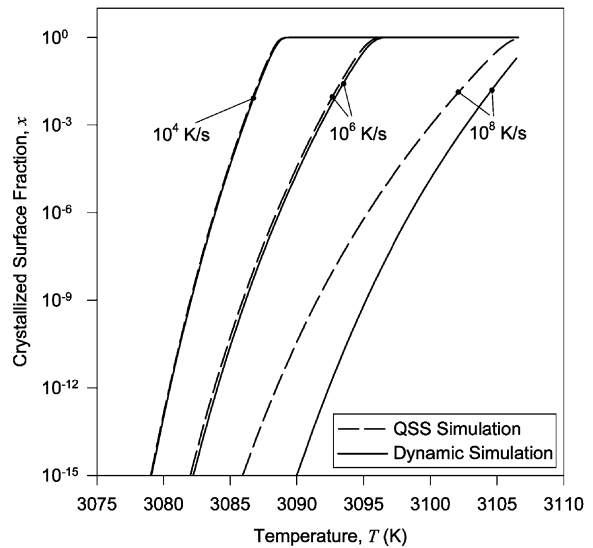


Fig. 9. Dynamic crystallization of graphite during peritectic melting of WC vs. temperature for various heating rates.

stable phase diagram in Fig. 1 suggests that if graphite surface crystallization is not completed by 3107 K, metastability will prevail, which implies that the WC substrate will melt and graphite nucleation would cease so that the transformed graphite would dissolve into the metastable melt. Hence, heating rates of order 10^8 K/s can be regarded as critical with respect to the peritectic melting reaction, as processing under higher rates would give rise to metastability.

7. Conclusions

Nucleation during peritectic melting constitutes a particularly interesting kinetic scenario, as it is associated with non-equilibration realized upon superheating rather than upon supercooling. In this study, a computational model was developed to simulate the kinetics of graphite nucleation upon WC superheating. The aim was to assess the importance of nucleation kinetics in limiting the rate of peritectic melting reaction upon annealing or continuous heating, and to examine the possibility of complete kinetic bypassing of the graphite phase.

The isothermal kinetic analysis suggests that

transformation time decreases monotonically with increasing superheat such that the minimum transformation time occurs at the metastable congruent melting point of WC. This is because increasing the superheat results in a decrease in both interfacial barriers and consequently nucleation and growth increase monotonically with temperature. Contrasting the dynamically computed kinetics against those computed by assuming steady state quantitatively demonstrates that nucleation transience influences the kinetics when annealing above 3090 K. According to the developed dynamic model graphitization becomes extremely rapid when annealing at high superheats; the transformation time for 1-ppm at the metastable melting point is computed to be ~ 2 ns.

The non-isothermal crystallization kinetics computed by means of cluster dynamics were contrasted against those computed by assuming quasi-static conditions for various heating rates, and they appear to deviate only in the case of 10^8 K/s, hence implying that nucleation transience influences the kinetics only under such ultra-high heating rates. The non-isothermal kinetic analysis suggests that under moderate to high heating rates (10^4 – 10^6 K/s) graphite transformation is completed at superheats of 40–50 K, while under ultra-high heating rates ($\sim 10^8$ K/s) the transformation remains incomplete by the time the metastable congruent melting point is attained. Therefore, under such highly non-equilibrium conditions the system cannot manage to kinetically respond to the induced deviation from equilibrium. The inadequacy in the system's kinetic response favors the prevalence of metastability and consequently thermodynamically favorable equilibration never manages to establish itself. Therefore, under such processing conditions, graphite nucleation would cease and the transfor-

med graphite would dissolve into the metastable melt. Hence heating rates of order 10^8 K/s can be considered as critical with respect to the peritectic melting reaction.

References

- [1] Figueredo AM, Cima MJ, Flemings MC, Haggerty JSM. *Metall Mater Trans A* 1994;25A:1747.
- [2] Misture ST, Matheis DP, Snyder RL, Blanton TN, Zorn GM, Seebacher B. *Physica C* 1995;250:175.
- [3] Kuznetsov VM, Oleinikov NN, Baranov AN, Tretyakov YD. *Inorg Mater* 1996;32:900.
- [4] Wei Lo DA, Cardwell DA, Dewhurst CD, Dung SL. *J Mater Res* 1996;11:786.
- [5] Kim CJ, Kim KB, Hong GW. *Physica C* 1994;243:366.
- [6] Perepezko JH, Boettinger WJ. *Mat Res Soc Symp Proc* 1983;19:223.
- [7] Gustafson PM. *Mater Sci Tech* 1986;2:653.
- [8] Angilello J, Thompson RD, Tu KN. *J Appl Crystallogr* 1989;22:523.
- [9] Demetriou M.D., Ghoniem N.M., Lavine A.S. *J Phase Equilib* 2002;23:305.
- [10] Rudy E. Report AFML-TR-65-2, Part V, 1969, Wright-Patterson Air Force Base, OH.
- [11] Thompson CV, Spaepen F. *Acta Metall* 1983;31:2021.
- [12] Hunziker O, Vandyoussefi M, Kurz W. *Acta Mater* 1998;18:6325.
- [13] Eustathopoulos N, Pique D. *Scripta Metall* 1980;14:1291.
- [14] Greer AL, Evans PV, Hamerton RG, Shangguan DK. *J Cryst Growth* 1990;99:38.
- [15] Spaepen FA. *Acta Metall* 1975;23:729.
- [16] Battezzati L, Antonione C, Riontino G. *J Non-Cryst Solids* 1987;89:114.
- [17] Moelwyn-Hughes EA. *Physical Chemistry*. Oxford: Pergamon Press, 1964.
- [18] Kelton KF, Greer AL, Thompson CV. *J Chem Phys* 1983;9:6261.
- [19] Demetriou MD, Ghoniem NM, Lavine AS. *Acta Mater* 2002;50:1421.
- [20] Demetriou M.D. Ph.D. dissertation, University of California, Los Angeles, 2001.
- [21] Kashchiev D. *Surf Sci* 1969;14:209.
- [22] Avrami MJ. *Chem Phys* 1940;8:212.
- [23] Shneidman VA. *J Chem Phys* 1995;103:9772.